SCIENTIFIC REPORTS

OPEN

Received: 21 October 2016
Accepted: 08 January 2017
Published: 10 February 2017

Ultrasensitive Label-free Electrochemical Immunosensor based on Multifunctionalized Graphene Nanocomposites for the Detection of Alpha Fetoprotein

Yaoguang Wang, Yong Zhang, Dan Wu, Hongmin Ma, Xuehui Pang, Dawei Fan, Qin Wei & Bin Du

In this work, a novel label-free electrochemical immunosensor was developed for the quantitative detection of alpha fetoprotein (AFP). Multifunctionalized graphene nanocomposites (TB-Au-Fe_3O_4-rGO) were applied to modify the electrode to achieve the amplification of electrochemical signal. TB-Au-Fe_3O_4-rGO includes the advantages of graphene, ferroferric oxide nanoparticles (Fe_3O_4 NPs), gold nanoparticles (Au NPs) and toluidine blue (TB). As a kind of redox probe, TB can produce the electrochemical signal. Graphene owns large specific surface area, high electrical conductivity and good adsorption property to load a large number of TB. Fe_3O_4 NPs have good electrocatalytic performance towards the redox of TB. Au NPs have good biocompatibility to capture the antibodies. Due to the good electrochemical performance of TB-Au-Fe_3O_4-rGO, the effective and sensitive detection of AFP was achieved by the designed electrochemical immunosensor. Under optimal conditions, the designed immunosensor exhibited a wide linear range from 1.0×10^{-5} ng/mL to 10.0 ng/mL with a low detection limit of 2.7 fg/mL for AFP. It also displayed good electrochemical performance including good reproducibility, selectivity and stability, which would provide potential applications in the clinical diagnosis of other tumor markers.

Alpha fetoprotein (AFP) is a tumor-associated fetal protein produced by the fetal liver and yolk sac[1]. The expressional level of AFP is highly elevated in hepatocellular carcinoma[2,3]. Therefore, AFP has been considered as one of the most important tumor markers in diagnosing and targeting of hepatocellular carcinoma[4]. A number of methods have been proposed for the quantitative detection of AFP, such as electrochemical immunoassay[5], photoelectrochemical immunoassay[6], fluoresencent immunoassay[7], chemiluminescent immunoassay[8] and enzyme-linked immunosorbent assay (ELISA)[9], etc. Compared with other methods, the electrochemical immunosensor has many advantages such as economical, sensitive, portable and simple-to-operate[10–13].

As a star among two-dimensional nanomaterials, graphene has attracted tremendous research interest in the field of electrochemistry due to their intrinsic properties, including the electronic, optical, and mechanical properties associated with their planar structure[14,15]. In general, the large specific surface area and the high electrical conductivity are the two key factors to promote the application of graphene in electrochemical immunosensors. For example, Tian *et al.* have developed chemically functionalized Ag/Au nanoparticles coated on graphene for the detection of carcinoembryonic antigen (CEA) in clinical immunoassay[16]. And Thavarungkul *et al.* have developed and tested a novel highly sensitive electrochemical immunosensor based on Au nanoparticles-graphene-chitosan nanocomposites[17]. Therefore, graphene-based electrochemical immunosensor can achieve a high sensitivity and a good stability[16–18]. In addition, graphene has another advantage of the good adsorption property[19,20], which is seldom developed and used in electrochemical immunosensors.

Key Laboratory of Chemical Sensing & Analysis in Universities of Shandong, School of Chemistry and Chemical Engineering, University of Jinan, Jinan 250022, P.R. China. Correspondence and requests for materials should be addressed to B.D. (email: dubin61@gmail.com)

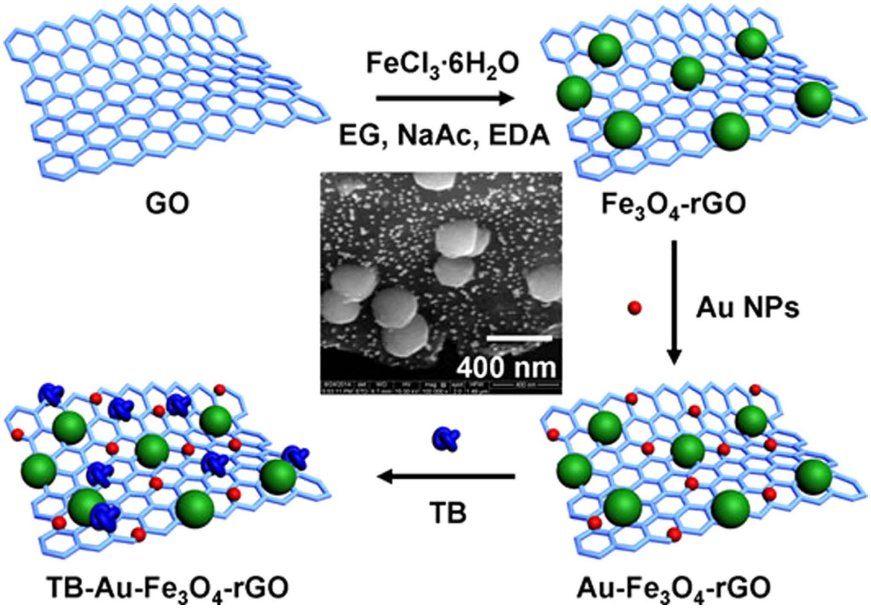

Figure 1. The synthesis procedure of the TB-Au-Fe_3O_4-rGO and SEM image of the Au-Fe_3O_4-rGO (inset).

According to our previous reports[21–24], reduced graphene oxide functionalized with ferroferric oxide (Fe_3O_4-rGO) can be used in adsorbing a variety of heavy metals. In this case, a label-free electrochemical immunosensor based on multifunctionalized graphene nanocomposites (TB-Au-Fe_3O_4-rGO) was designed for the quantitative detection of AFP. First of all, gold nanoparticles (Au NPs) which could immobilize the antibodies through the good biocompatibility were applied to functionalize the Fe_3O_4-rGO to obtain the Au-Fe_3O_4-rGO[25–35]. Subsequently, taking advantage of the good adsorption property, Au-Fe_3O_4-rGO was used to adsorb toluidine blue (TB) to obtain the TB-Au-Fe_3O_4-rGO. TB is a kind of organic dye and widely used as an electron transfer mediator for providing electrochemical signal in the electrochemical immunosensor[36]. As is known to all, ferroferric oxide nanoparticles (Fe_3O_4 NPs) have a good electrocatalytic performance[37–40], which can promote the redox of TB. In addition, the graphene can provide large specific surface area for the immobilization of antibodies and high electrical conductivity for the electron transfer. Therefore, the usage of the TB-Au-Fe_3O_4-rGO modified electrode to fabricate the electrochemical immunosensor can achieve the effective and sensitive detection of AFP.

Experimental

Apparatus and reagents. All electrochemical measurements were performed on a CHI760E electrochemical workstation (Huakeputian Technology Beijing Co., Ltd., China). A conventional three-electrode system was used for all electrochemical measurements: a glassy carbon electrode (GCE, 4 mm in diameter) as the working electrode, a saturated calomel electrode (SCE) as the reference electrode, and a platinum wire electrode as the counter electrode. Scanning electron microscope (SEM) images were obtained by using Quanta FEG250 field emission environmental SEM (FEI, United States) operated at 4 KV.

Human AFP and antibody to human AFP (anti-AFP) were purchased from Beijing Dingguo Changsheng Biotechnology Co., Ltd., China. Bovine serum albumin (BSA) and TB were purchased from Shanghai Sinopharm Chemical Reagent Co., Ltd., China. Sodium acetate trihydrate ($NaAc{\cdot}3H_2O$), chloroauric acid ($HAuCl_4{\cdot}4H_2O$) and trisodium citrate were purchased from Shanghai Aladdin Chemistry Co., Ltd, China. Ethanol, ethylene glycol (EG) and ethanediamine (EDA) were purchased from Tianjin Fuyu Fine Chemical Co., Ltd., China. Ferric chloride hexahydrate ($FeCl_3{\cdot}6H_2O$) was purchased from Tianjin Damao Chemical Reagent Co., Ltd., China. Phosphate buffered saline (PBS 1/15 M Na_2HPO_4 and KH_2PO_4) was used as an electrolyte for all electrochemical measurements, which was purged with nitrogen gas for 20 min to remove the dissolved oxygen. All other reagents were of analytical grade and ultrapure water was used throughout the study.

Synthesis of the TB-Au-Fe_3O_4-rGO. Figure 1 shows the synthesis procedure of the TB-Au-Fe_3O_4-rGO. SEM image was performed to characterize the shape and size of the Au-Fe_3O_4-rGO (inset of Fig. 1). Graphene oxide (GO) was synthesized by an improved Hummers method[41]. In brief, a mixture of concentrated H_2SO_4 (36 mL) and H_3PO_4 (4 mL) was added into a mixture of graphite flakes (0.3 g) and $KMnO_4$ (1.8 g), producing a slight exotherm to 35~40 °C. The reaction was then heated to 50 °C and stirred for 12 h. After that, the reaction was cooled to room temperature and poured onto ice (40 mL) with 30% H_2O_2 (0.3 mL), and the mixture was centrifuged and the supernatant was decanted away. For workup, the remaining solid material was washed in succession with water, 0.2 M HCl, ethanol and ether. The obtained solid was dried in vacuum overnight.

In a typical synthesis of Fe_3O_4-rGO[21]. $FeCl_3{\cdot}6H_2O$ (0.5 g) was dissolved in EG (10 mL) to form a clear solution, followed by the addition of NaAc (1.5 g), EDA (5 mL) and GO (0.5 g). The mixture was stirred vigorously for 30 min and then sealed in a teflon-lined stainless steel autoclave. The autoclave was heated to 200 °C and maintained for 8 h, and then was cooled to room temperature. The resulting black powder was washed several times

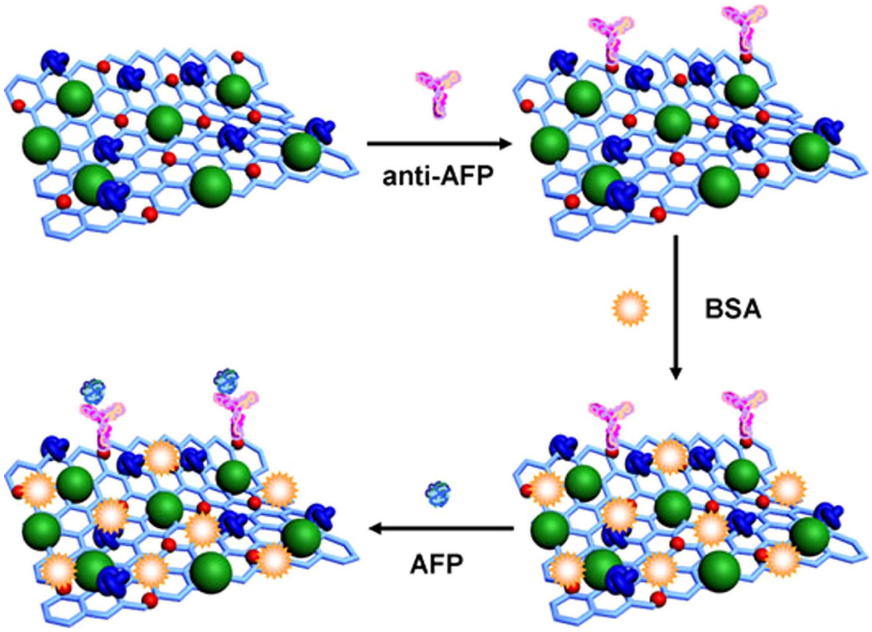

Figure 2. The schematic diagram of the label-free electrochemical immunosensor fabricated on the GCE.

and dried at 35 °C under high vacuum overnight. It should be noted that the GO was translated into the reduced graphene oxide (rGO) in the process of reaction.

Au NPs were synthesized by the classical Frens method[42]. In brief, a solution of $HAuCl_4$ (0.01 wt%, 100 mL) was heated to boiling, and then a solution of trisodium citrate (1 wt%, 1.5 mL) was added. The boiling solution turned a brilliant ruby-red in around 15 min, indicating the formation of Au NPs, and then it was cooled to room temperature.

A mixture of Fe_3O_4-rGO (20 mg) and the prepared Au NPs solution (40 mL) was shaked for 12 h, The resulting Au-Fe_3O_4-rGO was obtained by washed several times and dried at 35 °C under high vacuum overnight. 1 mL of 2 mg/mL Au-Fe_3O_4-rGO aqueous solution was mixed with 1 mL of 2 mg/mL TB solution under stirring for another 12 h. The final product was washed thoroughly and redispersed in 1 mL of water.

Fabrication of the immunosensor. Figure 2 shows the schematic diagram of the label-free electrochemical immunosensor fabricated on the GCE. A GCE was polished to a mirror-like finish with alumina powder (1.0, 0.3 and 0.05 μm), and then it was thoroughly cleaned before use. First, an aqueous solution of TB-Au-Fe_3O_4-rGO (2 mg/mL, 6 μL) was added onto the surface of bare GCE and then dried. After washed, anti-AFP dispersion (10 μg/mL, 6 μL) was added onto the electrode. According to the ref. 43, anti-AFP can be conjugated on the surface of TB-Au-Fe_3O_4-rGO due to the bonding between amino groups of antibodies and Au NPs. After incubated at 4 °C for 1 h and washed, BSA solution (10 mg/mL, 3 μL) was added onto the electrode to eliminate nonspecific binding sites. After incubated for another 1 h at 4 °C, the electrode was washed and incubated with a varying concentration of AFP ($1.0 \times 10^{-5} \sim 10.0$ ng/mL, 6 μL) for 1 h at room temperature, and then the electrode was washed extensively to remove unbounded AFP molecules for measurement. For Square Wave Voltammetry (SWV) to record the amperometric response in PBS at pH = 6.8, a detection potential from −0.6 V to 0 V was selected. The response time of one electrode is 30 seconds.

Results and Discussion

SEM and EDX characterization. Figure 3A shows SEM image of Au-Fe_3O_4-rGO. It can be observed that the rGO of Au-Fe_3O_4-rGO is thin and wrinkled, which resembles crumpled silk veil waves. The Fe_3O_4 NPs are loaded on the surface of rGO with an average diameter about 200 nm. A large number of Au NPs with an average size about 20 nm are successfully loaded on the surface of Fe_3O_4-rGO. EDX spectrum of Au-Fe_3O_4-rGO (Fig. 3B) was used to further explain what kinds of elements were contained in Au-Fe_3O_4-rGO. Al element can be observed because the sample was transferred on a clean aluminium foil for EDX analysis. Au-rGO and Fe_3O_4-rGO were also synthesized for the control experiments[44]. The Au-rGO retains the thin and wrinkled structure of rGO, which is loaded with massive Au NPs (Fig. 3C). In the SEM image of Fe_3O_4-rGO (Fig. 3D), the rGO presents lamellar fold structure and numbers of Fe_3O_4 NPs with a uniform diameter of about 200 nm are loaded on the surface of it.

Optimization of experimental conditions. In order to achieve an optimal electrochemical signal, optimizations of experimental conditions are necessary. The pH value of PBS and the concentration of TB-Au-Fe_3O_4-rGO influence the electrochemical current response. Figure 4A shows the different electrochemical current responses of the electrode modified with 2 mg/mL TB-Au-Fe_3O_4-rGO in different pH values of PBS for the detection of 10.0 ng/mL of AFP. Figure 4B shows the different electrochemical current responses of the electrode modified with different concentrations of TB-Au-Fe_3O_4-rGO in PBS at pH = 6.8 for the detection of

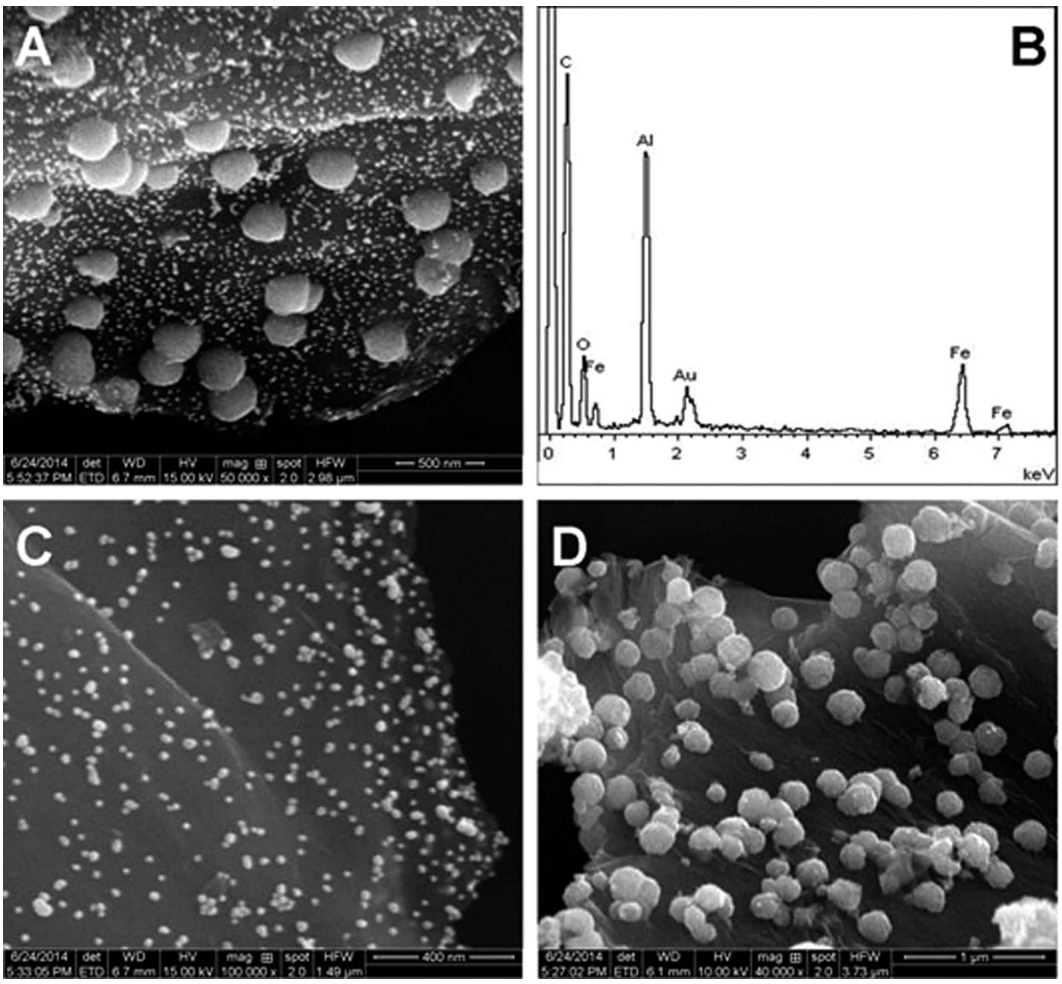

Figure 3. SEM images of Au-Fe_3O_4-rGO (**A**), Au-rGO (**C**) and Fe_3O_4-rGO (**D**); EDX spectrum of Au-Fe_3O_4-rGO (**B**).

10.0 ng/mL of AFP. As shown in these figures, the optimal amperometric response was achieved at a pH of 6.8 and at a concentration of 2 mg/mL. Therefore, PBS at pH = 6.8 and 2 mg/mL TB-Au-Fe_3O_4-rGO were selected for the test throughout this study.

In addition, the other factors were controlled strictly, for example, the incubation time was 1 h, the incubation temperature was the room temperature, and the concentration of antibodies was 10 μg/mL. All these above factors would make sure antibodies and antigens could effectively and specifically recognize with each other.

Electrochemical characterization. In order to investigate the role of TB, Fe_3O_4 NPs and Au NPs in the fabrication of the label-free electrochemical immunosensor, SWV curves of TB-Au-Fe_3O_4-rGO/GCE (curve a), TB-Au-rGO/GCE (curve b), TB-Fe_3O_4-rGO/GCE (curve c), anti-AFP/TB-Fe_3O_4-rGO/GCE (curve d) and Au-Fe_3O_4-rGO/GCE (e) were recorded in PBS at pH 6.8. As shown in Fig. 5A, Au-Fe_3O_4-rGO/GCE modified electrode has no obvious electrochemical current response (curve e). However, TB-Au-Fe_3O_4-rGO modified electrode (curve a) has an obvious electrochemical current response. It indicates that TB can produce the electrochemical current response for the immunosensor. In addition, TB-Au-rGO modified electrode (curve b) has an electrochemical current response about the half of TB-Au-Fe_3O_4-rGO modified electrode. It indicates that Fe_3O_4 NPs have a good electrocatalytical performance to promote the redox of TB. TB-Fe_3O_4-rGO modified electrode (curve c) has a slightly larger electrochemical current response than TB-Au-Fe_3O_4-rGO modified electrode. It indicates that Fe_3O_4-rGO can load more TB than Au-Fe_3O_4-rGO and the increase of the surface area cannot lead to the increase of electrochemical current response. But after modified with anti-AFP (curve d), the electrochemical current response has no obvious change. It indicates that anti-AFP cannot be captured on the surface of TB-Fe_3O_4-rGO without Au NPs. Therefore, Au NPs with a good biocompatibility can capture the antibodies.

SWV was also used to verify the successful fabrication of the immunosensor (Fig. 5B). It can be observed that the bare GCE (curve a) modified with TB exhibits an obvious electrochemical peak current at −0.24 V (curve b). After modified with anti-AFP (curve c), BSA (curve d) and AFP (curve e), the decreasing electrochemical current response indicates biological active substances can hinder the efficiency of electron transfer. The slight shift of the electrochemical peak potential might be due to the modification of the biological active substance.

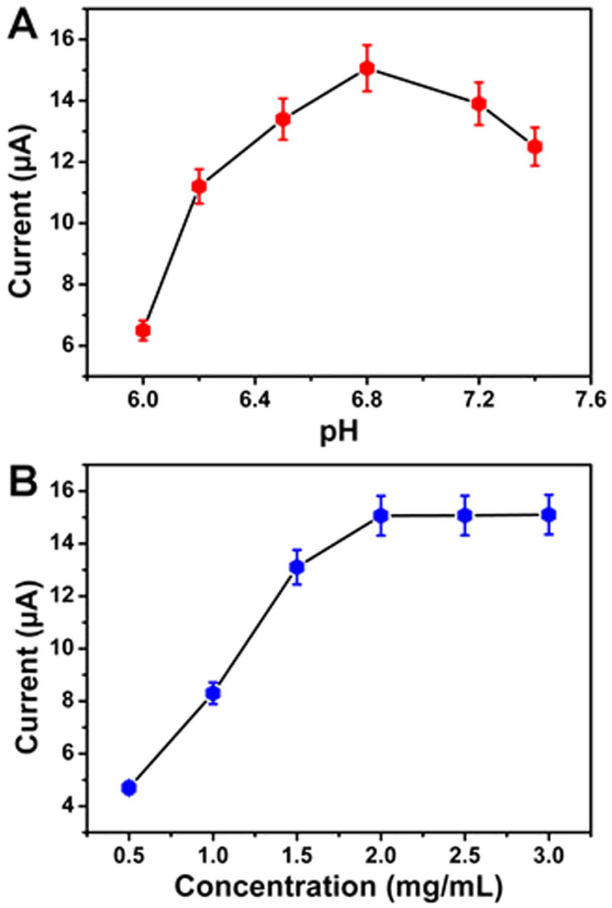

Figure 4. Effect of pH (**A**) and the concentration of TB-Au-Fe_3O_4-rGO (**B**) on the electrochemical current responses of the immunosensor for the detection of 10.0 ng/mL of AFP. Error bar = RSD ($n = 5$).

In order to further characterize the fabrication process of the label-free electrochemical immunosensor, Nyquist plots of the A.C. impedance method was recorded from 1 to 10^5 Hz at 0.2 V in a solution containing 0.1 M KCl and 2.5 mM $Fe(CN)_6^{3-}/Fe(CN)_6^{4-}$. Nyquist plots are consisted of two portions. The linear portion at low frequencies is associated with electrochemical behavior limited by diffusion. The semicircle portion at high frequencies is associated with the electrochemical process subject to electron transfer, where the diameter corresponds to the resistance. Simply, resistance change could be judged by observing the diameter change of semicircle portion. Thus, A.C. impedance is a suitable method for monitoring the changes in the surface features during the fabrication process[45–48]. The inset in Fig. 5C shows the Randles model for the equivalent circuit[49–51], which represents each component at the working electrode interface and in the solution during the electrochemical reaction in the presence of $Fe(CN)_6^{3-}/Fe(CN)_6^{4-}$: solution resistance ($R_s$), charge transfer resistance (R_{ct}), capacitance of double layer (C_{dl}), Warburg impedance (Z_w). As shown in the Fig. 5C, it can be observed that the bare GCE exhibits a very small resistance (curve a), which is characteristic of a diffusion-limiting step in the electrochemical process. After the modification of TB-Au-Fe_3O_4-rGO, the electrode shows a decreasing resistance (curve b). It implies that the successful immobilization of TB-Au-Fe_3O_4-rGO on the surface of bare GCE and TB-Au-Fe_3O_4-rGO can provide a sensitive interface to accelerate the electron transfer. The gradually increasing resistance of electrodes further modified with anti-AFP (curve c) and BSA (curve d) indicates the successful immobilization of the non-conductive bioactive substances. It also indicates that TB-Au-Fe_3O_4-rGO can offer a biocompatible surface for the capture of anti-AFP. After the modification of AFP, the electrode shows an increasing resistance (curve e), implying that the successful specific recognition between anti-AFP and AFP.

Characterization of the immunosensor. Under optimal conditions, the label-free electrochemical immunosensor was employed to detect different concentrations of AFP. Figure 6A shows the electrocatalytic current responses of the designed immunosensor for the detection of AFP covering the concentration range from 1.0×10^{-5} ng/mL (curve a) to 10.0 ng/mL (curve g). Figure 6B shows a linear relationship between electrocatalytic current responses and the logarithmic values of AFP concentration. The electrocatalytic current responses have a linear relationship with the logarithmic values of AFP concentration. And the linear regression equation of the calibration curve was $I = -0.62 \log C + 16.15$ with correlation coefficient of 0.99. According to the refs 52 and 53, the detection limit can be calculated with the equation of $c_L = 10^{(I-16.15)/-0.62}$, where c_L is the detection limit and I is given by the equation of $x_{b1} + 3s_{b1}$ (x_{b1} is the mean signal of blank measures, s_{b1} is the standard deviation of five

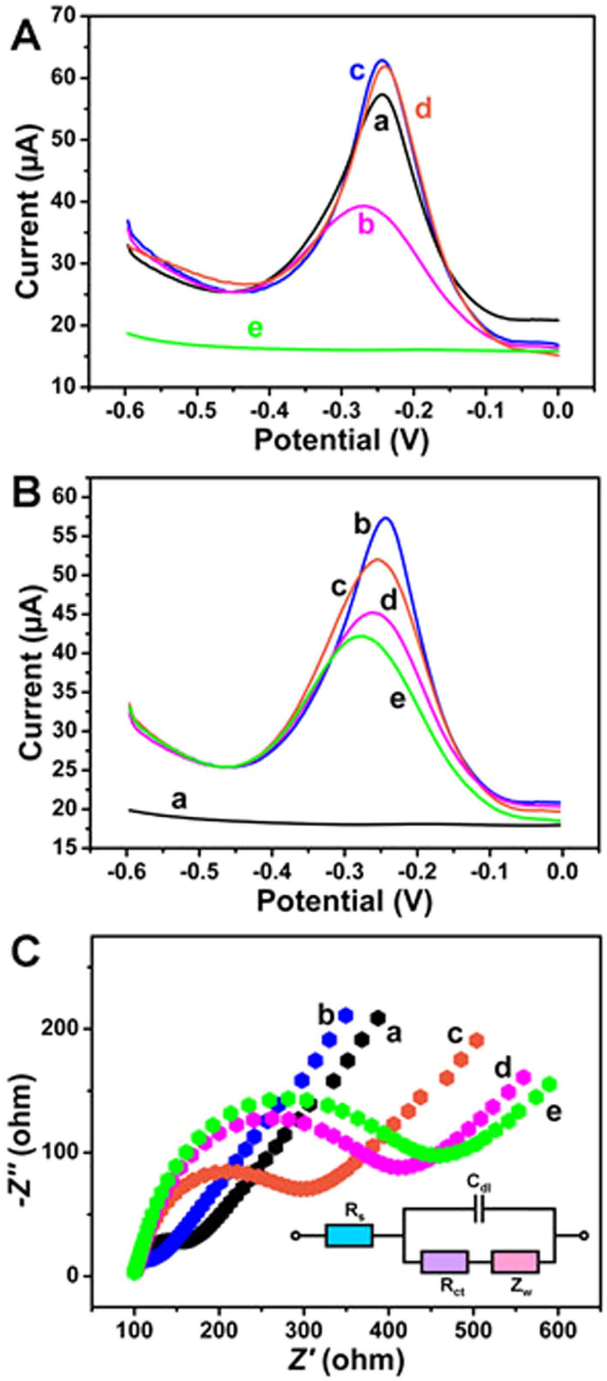

Figure 5. Electrochemical current responses recorded from −0.6 V to 0 V in PBS at pH 6.8 (**A**): TB-Au-Fe_3O_4-rGO/GCE (a), TB-Au-rGO/GCE (b), TB-Fe_3O_4-rGO/GCE (c), anti-AFP/TB-Fe_3O_4-rGO/GCE (d) and Au-Fe_3O_4-rGO/GCE (e); Electrochemical current responses recorded from −0.6 V to 0 V in PBS at pH 6.8 (**B**) and Nyquist plots of the A.C. impedance method (**C**): bare GCE (a), TB-Au-Fe_3O_4-rGO/GCE (b), anti-AFP/TB-Au-Fe_3O_4-rGO/GCE (c), BSA/anti-AFP/TB-Au-Fe_3O_4-rGO/GCE (d) and AFP/BSA/anti-AFP/TB-Au-Fe_3O_4-rGO/GCE (e); Inset shows the Randles model for the equivalent circuit, which represents each component at the working electrode interface and in the solution during the electrochemical reaction in the presence of $Fe(CN)_6^{3-}/Fe(CN)_6^{4-}$: solution resistance ($R_s$), electron transfer resistance (R_{ct}), capacitance of double layer (C_{dl}), Warburg impedance (Z_w).

parallel blank measures, the $x_{b1} = 19.50$ and $s_{b1} = 0.034$ in this work). The low detection limit of 2.7 fg/mL was obtained, which was ascribed to the novel signal amplification strategy based on multifunctionalized graphene nanocomposites in the fabrication of the designed immunosensor. The linear range and detection limit of the

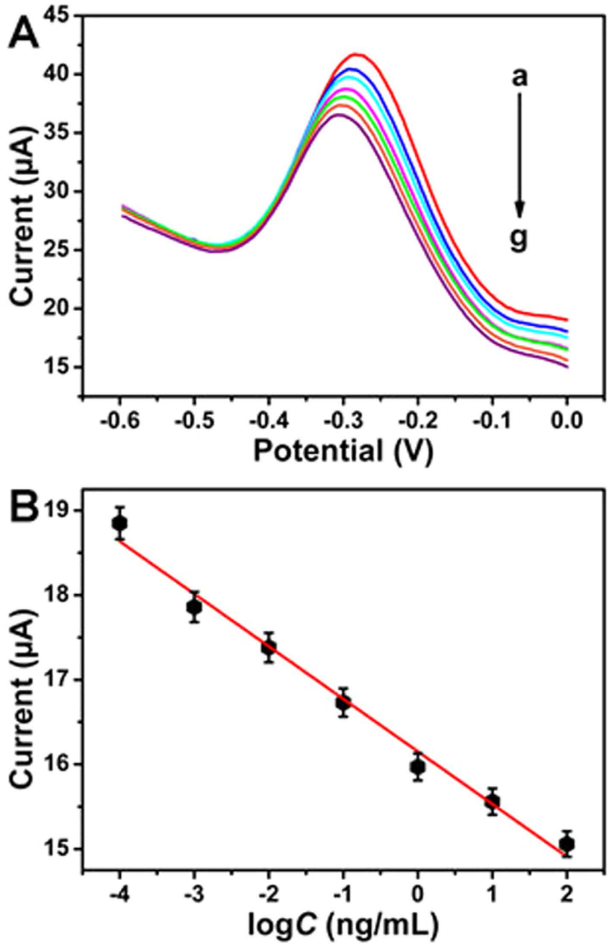

Figure 6. (**A**) Electrocatalytic current responses of the immunosensor for the detection of different concentrations of AFP: 1.0×10^{-5} ng/mL (a), 1.0×10^{-4} ng/mL (b), 1.0×10^{-3} ng/mL (c), 1.0×10^{-2} ng/mL (d), 0.1 ng/mL (e), 1.0 ng/mL (f) and 10.0 ng/mL (g); (**B**) Calibration curve of the immunosensor for the detection of different concentrations of AFP. Error bar = RSD ($n = 5$).

proposed immunosensor were compared with other reported methods for the detection of AFP in Table S1. It could be found that the proposed immunosensor showed a satisfactory linear range and detection limit.

Reproducibility, selectivity and stability. To evaluate the reproducibility of the label-free electrochemical immunosensor, a series of five electrodes were prepared for the detection of 1.0 ng/mL AFP (Fig. 7A). The relative standard deviation (RSD) of the measurements for the five electrodes was less than 5%, suggesting the precision and reproducibility of the designed immunosensor was quite good.

To investigate the specificity of the label-free electrochemical immunosensor, interference study was performed by using CEA, prostate specific antigen (PSA), human immunoglobulin (IgG) and BSA. 1.0 ng/mL AFP with and without 100.0 ng/mL interfering substances solution was measured by the designed immunosensor (Fig. 7B). It can be observed that the electrochemical current response variation due to the interfering substances was less than 5% of that without interferences, indicating the selectivity of the designed immunosensor was excellent.

To test the stability of the fabricated electrochemical immunosensor, it was stored at 4 °C when not in use. After one month, the electrochemical current response change was less than 5% for the detection of 1.0 ng/mL AFP. The good stability of the designed immunosensor can be ascribed to the good biocompatibility of the multifunctionalized graphene nanocomposites. The reproducibility, selectivity and stability of the designed immunosensor were all acceptable, thus it was suitable for quantitative detection of AFP in real human samples.

Real sample analysis. In order to validate the label-free electrochemical immunosensor, a comparative experiment with the commercialized available ELISA method for the detection of AFP in human serum sample was conducted (Table S2). The relative error between the two methods was in the range from −4.9% to 4.0%. These data revealed a good agreement between the two analytical methods, indicating the feasibility of the designed immunosensor for clinical application.

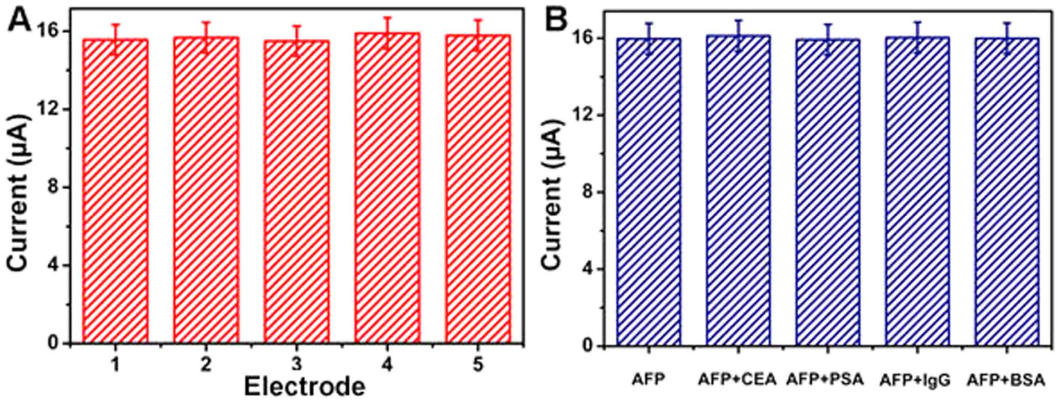

Figure 7. (**A**) Electrochemical signal responses of the immunosensor fabricated on five different electrodes for the detection of 1.0 ng/mL AFP; (**B**) Electrochemical signal responses of the immunosensor to 1.0 ng/mL AFP, 1.0 ng/mL AFP + 100 ng/mL CEA, 1.0 ng/mL AFP + 100.0 ng/mL PSA, 1.0 ng/mL AFP + 100.0 ng/mL IgG and 1.0 ng/mL AFP + 100.0 ng/mL BSA. Error bar = RSD ($n = 5$).

Conclusion

A novel label-free electrochemical immunosensor for the quantitative detection of AFP has been developed in this work. Thanks to the good adsorption property and the good electrochemical performance of the multifunctionalized graphene nanocomposites, the proposed immunosensor showed a wide linear range, a low detection limit, good reproducibility, fine selectivity and acceptable stability. The designed immunosensor might provide wide potential applications for the detection of AFP in clinical diagnosis and also can be applied in clinical detection of other tumor markers.

References

1. Won, Y. S. & Lee, S. W. Targeted retardation of hepatocarcinoma cells by specific replacement of alpha-fetoprotein RNA. *J. Biotechnol.* **129,** 614–619 (2007).
2. Otsuru, A., Nagataki, S., Koji, T. & Tamaoki, T. Analysis of alpha-fetoprotein gene expression in hepatocellular carcinoma and liver cirrhosis by *in situ* hybridization. *Cancer* **62,** 1105–1112 (1988).
3. Perz, J. F., Armstrong, G. L., Farrington, L. A., Hutin, Y. J. F. & Bell, B. P. The contributions of hepatitis B virus and hepatitis C virus infections to cirrhosis and primary liver cancer worldwide. *J. Hepatol.* **45,** 529–538 (2006).
4. Taketa, K. α-fetoprotein: Reevaluation in hepatology. *Hepatology* **12,** 1420–1432 (1990).
5. Kavosi, B., Hallaj, R., Teymourian, H. & Salimi, A. Au nanoparticles/PAMAM dendrimer functionalized wired ethyleneamine-viologen as highly efficient interface for ultra-sensitive α-fetoprotein electrochemical immunosensor. *Biosens. Bioelectron.* **59,** 389–396 (2014).
6. Xu, R. *et al.* A sensitive photoelectrochemical biosensor for AFP detection based on ZnO inverse opal electrodes with signal amplification of CdS-QDs. *Biosens. Bioelectron.* **74,** 411–417 (2015).
7. Xie, Q. *et al.* A sensitive fluorescent sensor for quantification of alpha-fetoprotein based on immunosorbent assay and click chemistry. *Biosens. Bioelectron.* **77,** 46–50 (2016).
8. Yang, X. Y., Guo, Y. S., Bi, S. & Zhang, S. S. Ultrasensitive enhanced chemiluminescence enzyme immunoassay for the determination of α-fetoprotein amplified by double-codified gold nanoparticles labels. *Biosens. Bioelectron.* **24,** 2707–2711 (2009).
9. Lee, Y. M., Jeong, Y., Kang, H. J., Chung, S., J. & Chung, B. H. Cascade enzyme-linked immunosorbent assay (CELISA). *Biosens. Bioelectron.* **25,** 332–337 (2009).
10. Sharma, M. K., Narayanan, J., Upadhyay, S. & Goel, A. K. Electrochemical immunosensor based on bismuth nanocomposite film and cadmium ions functionalized titanium phosphates for the detection of anthrax protective antigen toxin. *Biosens. Bioelectron.* **74,** 299–304 (2015).
11. Zhang, S. *et al.* Copper-doped titanium dioxide nanoparticles as dual-functional labels for fabrication of electrochemical immunosensors. *Biosens. Bioelectron.* **59,** 335–341 (2014).
12. Ilkhani, H., Sarparast, M., Noori, A., Bathaie, S. Z. & Mousavi, M. F. Electrochemical aptamer/antibody based sandwich immunosensor for the detection of EGFR, a cancer biomarker, using gold nanoparticles as a signaling probe. *Biosens. Bioelectron.* **74,** 491–497 (2015).
13. Pandiaraj, M., Sethy, N. K., Bhargava, K., Kameswararao, V. & Karunakaran, C. Designing label-free electrochemical immunosensors for cytochrome c using nanocomposites functionalized screen printed electrodes. *Biosens. Bioelectron.* **54,** 115–121 (2014).
14. Song, Y. *et al.* Recent advances in electrochemical biosensors based on graphene two-dimensional nanomaterials. *Biosens. Bioelectron.* **76,** 195–212 (2016).
15. Pei, H. *et al.* A graphene-based sensor array for high-precision and adaptive target identification with ensemble aptamers. *J. Am. Chem. Soc.* **134,** 13843–13849 (2012).
16. Huang, J., Tian, J., Zhao, Y. & Zhao, S. Ag/Au nanoparticles coated graphene electrochemical sensor for ultrasensitive analysis of carcinoembryonic antigen in clinical immunoassay. *Sensor. Actuat. B-Chem.* **206,** 570–576 (2015).
17. Samanman, S., Numnuam, A., Limbut, W., Kanatharana, P. & Thavarungkul, P. Highly-sensitive label-free electrochemical carcinoembryonic antigen immunosensor based on a novel Au nanoparticles-graphene-chitosan nanocomposite cryogel electrode. *Anal. Chim. Acta* **853,** 521–532 (2015).
18. Li, H., He, J., Li, S. & Turner, A. P. F. Electrochemical immunosensor with N-doped graphene-modified electrode for label-free detection of the breast cancer biomarker CA 15-3. *Biosens. Bioelectron.* **43,** 25–29 (2012).
19. Luo, K., Mu, Y., Wang, P. & Liu, X. Effect of oxidation degree on the synthesis and adsorption property of magnetite/graphene nanocomposites. *Appl. Surf. Sci.* **359,** 188–195 (2015).
20. Moussavi, G., Hossaini, Z. & Pourakbar, M. High-rate adsorption of acetaminophen from the contaminated water onto double-oxidized graphene oxide. *Chem. Eng. J.* **287,** 665–673 (2016).

21. Guo, X. *et al.* Synthesis of amino functionalized magnetic graphenes composite material and its application to remove Cr(VI), Pb(II), Hg(II), Cd(II) and Ni(II) from contaminated water. *J. Hazard. Mater.* **278,** 211–220 (2014).
22. Cui, L. *et al.* EDTA functionalized magnetic graphene oxide for removal of Pb (II), Hg (II) and Cu (II) in water treatment: Adsorption mechanism and separation property. *Chem. Eng. J.* **281,** 1–10 (2015).
23. Cui, L. *et al.* Removal of mercury and methylene blue from aqueous solution by xanthate functionalized magnetic graphene oxide: sorption kinetic and uptake mechanism. *J. Colloid Interf. Sci.* **439,** 112–120 (2015).
24. Wang, Y. *et al.* The removal of lead ions from aqueous solution by using magnetic hydroxypropyl chitosan/oxidized multiwalled carbon nanotubes composites. *J. Colloid Interf. Sci.* **451,** 7–14 (2015).
25. Peng, D., Liang, R. P., Huang, H. & Qiu, J. D. Electrochemical immunosensor for carcinoembryonic antigen based on signal amplification strategy of graphene and Fe_3O_4/Au NPs. *J. Electroanal. Chem.* **761,** 112–117 (2016).
26. Sun, G. *et al.* Paper-based electrochemical immunosensor for carcinoembryonic antigen based on three dimensional flower-like gold electrode and gold-silver bimetallic nanoparticles. *Electrochim. Acta* **147,** 650–656 (2014).
27. Fan, Y. *et al.* Highly sensitive impedimetric immunosensor based on single-walled carbon nanohorns as labels and bienzyme biocatalyzed precipitation as enhancer for cancer biomarker detection. *Biosens. Bioelectron.* **55,** 360–365 (2014).
28. Zhang, H., Liu, L., Fu, X. & Zhu, Z. Microfluidic beads-based immunosensor for sensitive detection of cancer biomarker proteins using multienzyme-nanoparticle amplification and quantum dotslabels. *Biosens. Bioelectron.* **42,** 23–30 (2013).
29. Gao, Z. D., Guan, F. F., Li, C. Y., Liu, H. F. & Song, Y. Y. Signal-amplified platform for electrochemical immunosensor based on TiO_2 nanotube arrays using a HRP tagged antibody-Au nanoparticles as probe. *Biosens. Bioelectron.* **41,** 771–775 (2013).
30. Rezaei, B., Khayamian, T., Majidi, N. & Rahmani, H. Immobilization of specific monoclonal antibody on Au nanoparticles for hGH detection by electrochemical impedance spectroscopy. *Biosens. Bioelectron.* **25,** 395–399 (2009).
31. Pei, H. *et al.* A DNA Nanostructure-based Biomolecular Probe Carrier Platform for Electrochemical Biosensing. *Adv. Mater.* **22,** 4754–4758 (2010).
32. Pei, H. *et al.* Regenerable electrochemical immunological sensing at DNA nanostructure-decorated gold surfaces. *Chem. Commun.* **47,** 6254–6256 (2011).
33. Yao, G. *et al.* Clicking DNA to gold nanoparticles: poly-adenine-mediated formation of monovalent DNA-gold nanoparticle conjugates with nearly quantitative yield. *NPG Asia Mater.* **7,** e159 (2015).
34. Pei, H., Zuo, X., Zhu, D., Huang, Q. & Fan, C. Functional DNA nanostructures for theranostic applications. *Accounts Chem. Res.* **47,** 550–559 (2014).
35. Pei, H. *et al.* Designed diblock oligonucleotide for the synthesis of spatially isolated and highly hybridizable functionalization of DNA-gold nanoparticle nanoconjugates. *J. Am. Chem. Soc.* **134,** 11876–11879 (2012).
36. Yao, Y. L. & Shiu, K. K. Low potential detection of glucose at carbon nanotube modified glassy carbon electrode with electropolymerized poly(toluidine blue O) film. *Electrochim. Acta* **53,** 278–284 (2007).
37. Qiu, J. D., Xiong, M., Liang, R. P., Peng, H. P. & Liu, F. Synthesis and characterization of ferrocene modified Fe_3O_4@Au magnetic nanoparticles and its application. *Biosens. Bioelectron.* **24,** 2649–2653 (2009).
38. Liu, X., Zhu, H. & Yang, X. An amperometric hydrogen peroxide chemical sensor based on graphene-Fe_3O_4 multilayer films modified ITO electrode. *Talanta* **87,** 243–248 (2011).
39. Wang, H. *et al.* β-Cyclodextrin/Fe_3O_4 hybrid magnetic nano-composite modified glassy carbon electrode for tryptophan sensing. *Sensor. Actuat. B-Chem.* **163,** 171–178 (2012).
40. Yari, A. & Derki, S. New MWCNT-Fe_3O_4@PDA-Ag nanocomposite as a novel sensing element of an electrochemical sensor for determination of Guanine and Adenine contents of DNA. *Sensor. Actuat. B-Chem.* **227,** 456–466 (2016).
41. Marcano, D. C. *et al.* Improved synthesis of graphene oxide. *ACS Nano* **4,** 4806–4814 (2010).
42. Frens, G. Controlled Nucleation for the Regulation of the Particle Size in Monodisperse Gold Suspensions. *Nature* **241,** 20–22 (1973).
43. Zhang, R., Hummelgård, M. & Olin, H. Simple synthesis of clay-gold nanocomposites with tunable color. *Langmuir* **26,** 5823–5828 (2010).
44. Wang, Y. *et al.* Ultrasensitive sandwich-type electrochemical immunosensor based on dual signal amplification strategy using multifunctional graphene nanocomposites as labels for quantitative detection of tissue polypeptide antigen. *Sensor. Actuat. B-Chem.* **214,** 124–131 (2015).
45. Lu, W. *et al.* A novel label-free amperometric immunosensor for carcinoembryonic antigen based on Ag nanoparticle decorated infinite coordination polymer fibres. *Biosens. Bioelectron.* **57,** 219–225 (2014).
46. Li, F., Feng, Y., Dong, P., Yang, L. & Tang, B. Gold nanoparticles modified electrode via simple electrografting of *in situ* generated mercaptophenyl diazonium cations for development of DNA electrochemical biosensor. *Biosens. Bioelectron.* **26,** 1947–1952 (2011).
47. Li, F., Yang, L., Chen, M., Qian, Y. & Tang, B. A novel and versatile sensing platform based on HRP-mimicking DNAzyme-catalyzed template-guided deposition of polyaniline. *Biosens. Bioelectron.* **41,** 903–906 (2013).
48. Li, F., Feng, Y., Dong, P. & Tang, B. Gold nanoparticles modified electrode via a mercapto-diazoaminobenzene monolayer and its development in DNA electrochemical biosensor. *Biosensors and Bioelectronics* **25,** 2084–2088 (2010).
49. Bhalla, V., Sharma, P., Pandey, S. K. & Suri, C. R. Impedimetric label-free immunodetection of phenylurea class of herbicides. *Sensor. Actuat. B-Chem.* **171–172,** 1231–1237 (2012).
50. Hayat, A., Barthelmebs, L. & Marty, J. L. Electrochemical impedimetric immunosensor for the detection of okadaic acid in mussel sample. *Sensor. Actuat. B-Chem.* **171–172,** 810–815 (2012).
51. Han, T. *et al.* Gold nanoparticles enhanced electrochemiluminescence of graphite-like carbon nitride for the detection of Nuclear Matrix Protein 22. *Sensor. Actuat. B-Chem.* **205,** 176–183 (2014).
52. Fassel, V. Nomenclature, symbols, units and their usage in spectrochemical analysis—II. data interpretation Analytical chemistry division. *Spectrochim. Acta B* **33,** 241–245 (1978).
53. Ren, K., Wu, J., Yan, F., Zhang, Y. & Ju, H. Immunoreaction-triggered DNA assembly for one-step sensitive ratiometric electrochemical biosensing of protein biomarker. *Biosens. Bioelectron.* **66,** 345–349 (2015).

Acknowledgements

This study was supported by the National Natural Science Foundation of China (Nos 21375047, 21377046, 21575050 and 21505051), National Key Scientific Instrument and Equipment Development Project of China (No. 21627809), the Science and Technology Development Plan of Shandong Province (No. 2014GSF120004), the Special Project for Independent Innovation and Achievements Transformation of Shandong Province (No. 2014ZZCX05101), and QW thanks the Special Foundation for Taishan Scholar Professorship of Shandong Province (No. ts20130937) and UJN.

Author Contributions

Y.W. and B.D. conceived and designed the experiments. Y.W. performed the experiments, analyzed the data and wrote the first draft of the manuscript. Y.Z., D.W., H.M., X.P., D.F. and Q.W. contributed substantially to revisions.

Additional Information

Supplementary information accompanies this paper at http://www.nature.com/srep

Competing financial interests: The authors declare no competing financial interests.

How to cite this article: Wang, Y. *et al.* Ultrasensitive Label-free Electrochemical Immunosensor based on Multifunctionalized Graphene Nanocomposites for the Detection of Alpha Fetoprotein. *Sci. Rep.* **7**, 42361; doi: 10.1038/srep42361 (2017).

Publisher's note: Springer Nature remains neutral with regard to jurisdictional claims in published maps and institutional affiliations.